# Improved Adaptive State-of-Charge Estimation for Batteries Using a Multi-model Approach

Fang, H.; Zhao, X.; Wang, Y.; Sahinoglu, Z.; Wada, T.; Hara, S.; de Callafon, R.A.

TR2014-005 May 15, 2014

**Abstract**

Adaptive estimation of the state-of-charge (SoC) for batteries is increasingly appealing, thanks to its ability to accommodate uncertain or time-varying model parameters. We propose to improve the adaptive SoC estimation using multiple models in this study, developing a unique algorithm called MM-AdaSoC. Specifically, two submodels in state-space form are generated from a modified Nernst battery model. Both are shown to be locally observable with admissible inputs. The iterated extended Kalman filter (IEKF) is then applied to each submodel in parallel, estimating simultaneously the SoC variable and unknown parameters. The SoC estimates obtained from the two separately implemented IEKFs are fused to yield the final overall SoC estimates, which tend to have higher accuracy than those obtained from a single-model. Its effectiveness is demonstrated using simulation and experiments. The notion of multi-model estimation can be extended promisingly to the development of many other advanced battery management and control strategies.

*Journal of Power Sources*

# Improved Adaptive State-of-Charge Estimation for Batteries Using a Multi-model Approach☆

Huazhen Fang[a], Xin Zhao[a], Yebin Wang[b], Zafer Sahinoglu[b], Toshihiro Wada[c], Satoshi Hara[c], Raymond A. de Callafon[a]

[a]*Department of Mechanical & Aerospace Engineering, University of California, San Diego, CA 92093, USA*
[b]*Mitsubishi Electric Research Laboratories, 201 Broadway, Cambridge, MA 02139, USA*
[c]*Advanced Technology R&D Center, Mitsubishi Electric Corporation, 8-1-1, Tsukaguchi-honmachi, Amagasaki City, 661-8661, Japan*

**Abstract**

Adaptive estimation of the state-of-charge (SoC) for batteries is increasingly appealing, thanks to its ability to accommodate uncertain or time-varying model parameters. We propose to improve the adaptive SoC estimation using *multiple models* in this study, developing a unique algorithm called `MM-AdaSoC`. Specifically, two submodels in state-space form are generated from a modified Nernst battery model. Both are shown to be locally observable with admissible inputs. The iterated extended Kalman filter (IEKF) is then applied to each submodel in parallel, estimating simultaneously the SoC variable and unknown parameters. The SoC estimates obtained from the two separately implemented IEKFs are fused to yield the final overall SoC estimates, which tend to have higher accuracy than those obtained from a single-model. Its effectiveness is demonstrated using simulation and experiments. The notion of multi-model estimation can be extended promisingly to the development of many other advanced battery management and control strategies.

*Keywords:*
State-of-charge, adaptive estimation, multiple models, state and parameter estimation, nonlinear observability, iterated extended Kalman filter

## 1. Introduction

Industrial applications of batteries usually require a well-designed management system for operational safety and performance, which monitors the running status and regulates the charging/discharging processes [1]. One of its fundamental functions is to estimate the state-of-charge (SoC), i.e., the percentage ratio of the present battery capacity over its maximum capacity.

☆Corresponding author Y. Wang. Tel: 001-617-621-7500; fax: 001-617-621-7550. Email address: yebin-wang@ieee.org

*Literature review:* SoC estimation has remained an active research field during the past years, and the reader may refer to [2] for a survey. A notable trend in this area is the increasing emphasis on model-based estimation methods. The dynamic models, derived from either equivalent circuits or electrochemical principles, facilitate the assimilation of the battery data and lead to real-time SoC estimation with bounded errors. While battery modeling has been well-accomplished [3], more attention is being geared towards the development of estimation algorithms. Application of the Kalman filtering (KF) techniques has been remarkable in this respect. The classical linear KF and its extensions to nonlinear systems, including the extended KF (EKF), unscented KF (UKF), iterated extended KF (IEKF), have been used to deal with SoC estimation based on electrochemical and equivalent circuit models, see [4–13]. A variety of other state observers originating from control approaches have also played a role in constructing SoC estimators. Here, we highlight the sliding mode observer [14], adaptive model reference observer [15], Lyapunov-based observer [16] and PDE-based observer [17, 18].

Since a good model is a prerequisite, model-based SoC estimation typically follows after the procedures of dynamic modeling and parameter identification. However, accurate identification is challenging. First, the parameters in a battery model are often subject to changes with time and operational conditions. For instance, the internal resistance will rise and the capacity diminish as a result of battery aging. Another example is the charging and discharging efficiencies, which are dependent on the SoC, magnitude of current and temperature. Second, the parameters may differ from one battery to another, making identification for each battery at least rather cumbersome. Therefore, adaptive approaches are more desirable, merging both identification and SoC estimation in one step. As shown in Fig. 1, an adaptive SoC estimator gives not only the SoC estimates but also the estimates of the model parameters in real time after assimilating the current-voltage data on the basis of a model. The parameter estimates will then be used to update the model to aid the next-step estimation.

Adaptive SoC estimation has been attracting considerable attention in the recent literature. An adaptive EKF-based SoC estimator is designed in [9], which interacts with a parameter estimator. In [11], state augmentation is conducted to incorporate the SoC variable and model parameters, and then the UKF is applied to estimate the augmented state. However, the convergence, and as a result, the accuracy, are noted to be difficult to guarantee. In [13], an adaptive SoC estimator is developed using the IEKF, guided by an analysis of the observability/identifiability. Novel adaptive PDE observers for SoC estimation have also been reported in [19]. It should be noted that all these existing approaches are based on a single battery model, and here we instead propose to exploit multiple models for better estimation performance.

*Statement of contributions:* In this paper, we aim to achieve *adaptive, high-fidelity and easy-to-implement SoC estimation*. For this purpose, we seamlessly link the notion of 'multiple models' and adaptive SoC estimation. A multitude of models, compared to a single one, can give a better description of complicated uncertain dynamics [20–22], thus particularly suitable to deal with the tasks relevant to batteries. The design of the adaptive SoC estimator partially builds on our previous work [13]. In that work, we propose an adaptive approach for SoC estimation via IEKF-based simultaneous state and parameter estimation. While credible estimation is observed, the accuracy is still limited in [13] by the mismatch between the model and the true system. This fact motivates the development of the `MM-AdaSoC` algorithm in this paper.

An overview of the construction of `MM-AdaSoC` is as follows. First, multiple submodels are brought up from a modified Nernst battery model by fixing some parameters and assuming the others unknown. Each submodel is shown locally observable with admissible inputs by rigorous analysis. Then, an adaptive SoC estimation scheme will be implemented simultaneously but separately to each submodel, with the submodel in each implementation assumed true. The SoC estimates resulting from different submodels will be fused in the light of a certain strategy to obtain the final estimate. As such, we boost the accuracy of SoC estimation despite the presence of uncertainties plaguing battery models.

The main contributions of this paper lie in two aspects. First, this is the first known study of multi-model adaptive SoC estimation to the best of our knowledge, and it is shown that the proposed `MM-AdaSoC` algorithm provides more accurate estimation while maintaining a good balance over the computational cost. Second, we introduce the multi-model framework for battery management and control. In addition to the proposed `MM-AdaSoC`, we discuss various other ways for SoC estimation enhanced by multiple models. Many more battery management strategies involving estimation and control can also be improved on a multi-model basis.

*Organization:* The rest of the paper is organized follows. Section 2 presents a basic review of the multi-model estimation theory. Section 3 describes the model construction and gives observability analysis. Section 4 incorporates adaptive SoC estimation and multi-model estimation to establish the `MM-AdaSoC` algorithm, the effectiveness of which is validated in Section 5 by simulation and experimental results. Finally, Section 6 gathers our conclusions and ideas for future work.

## 2. Basics of Multi-model Estimation

The structure of a typical multi-model estimator is shown in Fig. 2. In this section, we give a review of the multi-model estimation, with an emphasis on the estimate fusion strategy.

Its first part is composed of a bank of parallel filters based on different models. Each filter assimilates the data to produce its own estimate. All the estimates will then be fused to give the best estimate. Many options exist for the elemental filter, such as the KF for a linear model or the EKF for a nonlinear one. What is of particular interest here is the design of the fusion strategy.

Let us consider a general system. Its unknown state at time instant $k$ is denoted by $\mathbf{x}_k \in \mathbb{R}^{n_\mathbf{x}}$ and its measurement by $\mathbf{z}_k \in \mathbb{R}^{n_\mathbf{z}}$. Different models are available to describe the system, leading to a model set $\mathbb{M} = \{\mathscr{M}_1, \mathscr{M}_2, \cdots, \mathscr{M}_N\}$. Suppose that $\mathscr{M}_i$ is given by

$$\mathscr{M}_i : \begin{cases} \mathbf{x}_{k+1} = \mathbf{f}^i(\mathbf{x}_k) + \mathbf{w}_k^i, \\ \mathbf{z}_k = \mathbf{h}^i(\mathbf{x}_k) + \mathbf{v}_k^i, \end{cases} \tag{1}$$

where $\mathbf{f}^i$ and $\mathbf{h}^i$ are $C^1$ functions to represent the state transition and measurement, respectively, and $\{\mathbf{w}_k^i\}$ and $\{\mathbf{v}_k^i\}$ are uncorrelated, zero-mean, white Gaussian noise sequences with covariances $\mathbf{Q}_k^i \geq 0$ and $\mathbf{R}_k^i > 0$, respectively. While assuming that the true system coincides with one model at each time instant, we do not know which model matches the system at any time. Thus a probabilistic description is used. Let $s_k$ denote the system running status at $k$. It may take any $\mathscr{M}_i$ for $i = 1, 2, \cdots, N$ to address the uncertainty of model matching. The probability of the event $s_k = \mathscr{M}_i$ is denoted as $p(s_k = \mathscr{M}_i)$, or simply, $p(s_k^i)$. In other words, $p(s_k^i)$ indicates the *a priori* probability that the true model is $\mathscr{M}_i$ at time $k$. Obviously, $\sum_{i=1}^N p(s_k^i) = 1$.

From a statistical perspective, $\mathbf{x}_k$ and $\mathbf{z}_k$ are continuous random variables and $s_k$ a discrete one. Without causing confusion, we use the symbol $p$ to denote the probability density function (pdf), probability mass function (pmf) or mixed pdf-pmf in the sequel for convenience. We define the information set as $\mathbb{Z}_k = \{\mathbf{z}_1, \mathbf{z}_2, \cdots, \mathbf{z}_k\}$ and intend to estimate $\mathbf{x}_k$ from $\mathbb{Z}_k$, hence considering $p(\mathbf{x}_k|\mathbb{Z}_k)$. By the Bayes' theorem, we have

$$\begin{aligned} p(\mathbf{x}_k|\mathbb{Z}_k) &= \sum_{i=1}^N p(\mathbf{x}_k, s_k^i|\mathbb{Z}_k) \\ &= \sum_{i=1}^N p(\mathbf{x}_k|s_k^i, \mathbb{Z}_k) p(s_k^i|\mathbb{Z}_k). \end{aligned} \tag{2}$$

When $p(\mathbf{x}_k|\mathbb{Z}_k)$ becomes available, we can carry out minimum-mean-square-error (MMSE) estimation or Maximum a Posteriori (MAP) estimation of $\mathbf{x}_k$:

$$\text{MMSE:} \quad \hat{\mathbf{x}}_{k|k} = \mathrm{E}(\mathbf{x}_k|\mathbb{Z}_k) = \int \mathbf{x}_{k|k} p(\mathbf{x}_k|\mathbb{Z}_k) \mathrm{d}\mathbf{x}_k,$$

$$\text{MAP:} \quad \hat{\mathbf{x}}_{k|k} = \arg\max_{\mathbf{x}_k} p(\mathbf{x}_k|\mathbb{Z}_k).$$

Independent of the method (MMSE or MAP) used, it follows from (2) that

$$\hat{\mathbf{x}}_{k|k} = \sum_{i=1}^{N} \hat{\mathbf{x}}^i_{k|k} p(s^i_k|\mathbb{Z}_k), \tag{3}$$

where $\hat{\mathbf{x}}^i_{k|k}$ is the estimate of $\mathbf{x}_k$ based on the model $\mathscr{M}_i$. An observation from this analysis is that $p(s^i_k|\mathbb{Z}_k)$ turns out to be a probabilistic weight coefficient. The associated estimation error covariance is

$$\begin{aligned}
\mathbf{P}_{k|k} &= \mathrm{E}\left[ (\hat{\mathbf{x}}_k - \mathbf{x}_k)(\hat{\mathbf{x}}_k - \mathbf{x}_k)^\top \middle| \mathbb{Z}_k \right] \\
&= \int (\hat{\mathbf{x}}_k - \mathbf{x}_k)(\hat{\mathbf{x}}_k - \mathbf{x}_k)^\top p(\mathbf{x}_k|\mathbb{Z}_k) \mathrm{d}\mathbf{x}_k \\
&= \sum_{i=1}^{N} \int (\hat{\mathbf{x}}_k - \mathbf{x}_k)(\hat{\mathbf{x}}_k - \mathbf{x}_k)^\top p(\mathbf{x}_k, s^i_k|\mathbb{Z}_k) \mathrm{d}\mathbf{x}_k \\
&= \sum_{i=1}^{N} \int (\hat{\mathbf{x}}_k - \mathbf{x}_k)(\hat{\mathbf{x}}_k - \mathbf{x}_k)^\top p(\mathbf{x}_k|s^i_k, \mathbb{Z}_k) \mathrm{d}\mathbf{x}_k p(s^i_k|\mathbb{Z}_k) \\
&= \sum_{i=1}^{N} \left[ \mathbf{P}^i_{k|k} + (\hat{\mathbf{x}}_k - \hat{\mathbf{x}}^i_k)(\hat{\mathbf{x}}_k - \hat{\mathbf{x}}^i_k)^\top \right] p(s^i_k|\mathbb{Z}_k).
\end{aligned} \tag{4}$$

Let us take a closer look at $p(s^i_k|\mathbb{Z}_k)$. Using the Bayes' theorem again, we see that

$$\begin{aligned}
p(s^i_k|\mathbb{Z}_k) &= \frac{p(s^i_k, \mathbb{Z}_k)}{p(\mathbb{Z}_k)} \\
&= \frac{p(\mathbf{z}_k|s^i_k, \mathbb{Z}_{k-1}) p(s^i_k|\mathbb{Z}_{k-1})}{p(\mathbf{z}_k|\mathbb{Z}_{k-1})} \\
&= \frac{p(\mathbf{z}_k|s^i_k, \mathbb{Z}_{k-1}) p(s^i_k|\mathbb{Z}_{k-1})}{\sum_{j=1}^{N} p(\mathbf{z}_k, s^j_k|\mathbb{Z}_{k-1})} \\
&= \frac{p(\mathbf{z}_k|s^i_k, \mathbb{Z}_{k-1}) p(s^i_k|\mathbb{Z}_{k-1})}{\sum_{j=1}^{N} p(\mathbf{z}_k|s^j_k, \mathbb{Z}_{k-1}) p(s^j_k|\mathbb{Z}_{k-1})}.
\end{aligned} \tag{5}$$

Furthermore, we have

$$\begin{aligned}
p(\mathbf{z}_k|s^i_k, \mathbb{Z}_{k-1}) &= \int p(\mathbf{z}_k, \mathbf{x}_k|s^i_k, \mathbb{Z}_{k-1}) \mathrm{d}\mathbf{x}_k \\
&= \int p(\mathbf{z}_k|\mathbf{x}_k, s^i_k, \mathbb{Z}_{k-1}) p(\mathbf{x}_k|s^i_k, \mathbb{Z}_{k-1}) \mathrm{d}\mathbf{x}_k \\
&= \int p(\mathbf{z}_k|\mathbf{x}_k, s^i_k) p(\mathbf{x}_k|s^i_k, \mathbb{Z}_{k-1}) \mathrm{d}\mathbf{x}_k.
\end{aligned}$$

Under the mildly simplified assumption that $p(\mathbf{z}_k|\mathbf{x}_k, s_k^i) = \mathscr{N}\left(\mathbf{h}^i(\mathbf{x}_k), \mathbf{R}_k^i\right)$ and $p(\mathbf{x}_k|s_k^i, \mathbb{Z}_{k-1}) = \mathscr{N}\left(\hat{\mathbf{x}}_{k|k-1}^i, \mathbf{P}_{k|k-1}^i\right)$, $p(\mathbf{z}_k|s_k^i, \mathbb{Z}_{k-1})$ can be approximated as

$$p(\mathbf{z}_k|s_k^i, \mathbb{Z}_{k-1}) \approx (2\pi)^{-\frac{n_\mathbf{z}}{2}} \left|\mathbf{S}_k^i\right|^{-\frac{1}{2}} \exp\left[-\frac{1}{2}(\tilde{\mathbf{z}}_k^i)^\top |\mathbf{S}_k^i|^{-1} \tilde{\mathbf{z}}_k^i\right],$$

where

$$\begin{aligned}
\tilde{\mathbf{z}}_k^i &= \mathbf{z}_k - \mathbf{h}^i(\hat{\mathbf{x}}_{k|k-1}^i), \\
\mathbf{S}_k^i &= \mathbf{H}_k^i \mathbf{P}_{k|k-1}^i (\mathbf{H}_k^i)^\top + \mathbf{R}_k^i, \\
\mathbf{H}_k^i &= \frac{\partial \mathbf{h}^i}{\partial \mathbf{x}} \left(\hat{\mathbf{x}}_{k|k-1}^i\right).
\end{aligned}$$

Furthermore,

$$p(s_k^i|\mathbb{Z}_{k-1}) = \frac{p(\mathbb{Z}_{k-1}|s_k^i)p(s_k^i)}{p(\mathbb{Z}_{k-1})} = p(s_k^i),$$

since $p(\mathbb{Z}_{k-1}|s_k^i) = 1$ and $p(\mathbb{Z}_{k-1}) = 1$ because $\mathbb{Z}_{k-1}$ is an event with probability 1 at time $k-1$. If we define $\mu_k^i = p(s_k^i|\mathbb{Z}_k)$ and $w_k^i = p(\mathbf{z}_k|s_k^i, \mathbb{Z}_{k-1})$ and suppose $\pi_k^i = p(s_k^i)$, (5) becomes

$$\mu_k^i = \frac{w_k^i \pi_k^i}{\sum_{j=1}^N w_k^j \pi_k^j}. \tag{6}$$

Hence, by (3)-(4), the fusion strategy, or the fuser as is called, is given by

$$\hat{\mathbf{x}}_{k|k} = \sum_{i=1}^N \hat{\mathbf{x}}_{k|k}^i \mu_k^i, \tag{7}$$

$$\mathbf{P}_{k|k} = \sum_{i=1}^N \left[\mathbf{P}_{k|k}^i + (\hat{\mathbf{x}}_k - \hat{\mathbf{x}}_k^i)(\hat{\mathbf{x}}_k - \hat{\mathbf{x}}_k^i)^\top\right] \mu_k^i. \tag{8}$$

The final conclusion drawn from this analysis is as follows: the fused estimate (covariance) is a linear weighted combination of the estimates from the elemental filters. It can be noted that

- The estimation is based on a series of elemental filters and the fusion. The process is similar to a ‘ weight-based reconciliation’, which balances the role that different models potentially play in the estimation task.

- The residuals of the elemental filter based on the ‘correct’ model that best match the true system is expected to be remarkably smaller than those of the others [20]. As a result, the probabilistic weight associated to this filter, say, $\mu_k^*$, will tend to increase and downplay the others. The fused estimate will approach the estimate based on the correct model.

## 3. Battery Models and Observability Analysis

We investigate the battery modeling in this section. We first develop two submodels from a slightly modified Nernst model and then analyze the local observability properties for each one.

### *3.1. Construction of Multiple Battery Models*

A battery model consists of a set of equations that relate the input (charging/discharging current), the state variables (e.g., SoC) and the output(terminal voltage). Various models have been proposed and used, depending on the specific purposes. For SoC estimation, we consider the Nernst model here [5]:

$$y_k = K_1 + K_2 \ln(\mathrm{SoC}_k) + K_3 \ln(1 - \mathrm{SoC}_k) - Ru_k, \tag{9}$$

where $y_k$ is the terminal voltage at time instant $k$, $u_k$ is the applied current ($u > 0$ for discharging and $u < 0$ for charging), $R$ is the internal resistance, and $K_i$ for $i = 1, 2, 3$ are constants. To make (9) more capable of grasping the dynamics of certain batteries, we propose the following modification:

$$y_k = K_1 + K_2 \ln(\tau_1 + \mathrm{SoC}_k) + K_3 \ln(\tau_2 + 1 - \mathrm{SoC}_k) - Ru_k, \tag{10}$$

where two additional constants $\tau_1$ and $\tau_2$ are added. In above, $K_1 + K_2 \ln(\tau_1 + \mathrm{SoC}_k) + K_3 \ln(\tau_2 + 1 - \mathrm{SoC}_k)$ in (10) can be regarded as the open-circuit voltage (OCV) term. The dynamic change of the SoC is described by the integration of the current over time. In the discrete time, it is given by

$$\mathrm{SoC}_k = \mathrm{SoC}_0 - \sum_{i=0}^{k-1} \frac{\eta \cdot \Delta T}{C_0} u_i,$$

where $\eta$ is the Coulombic efficiency, $C_0$ the nominal capacity in ampere-hour (Ah), and $\Delta T$ is the sampling period. An equivalent difference equation is

$$\mathrm{SoC}_{k+1} = \mathrm{SoC}_k - K_0 u_k, \tag{11}$$

where $K_0 = \eta \cdot \Delta T / C_0$. We then obtain a state-space model for batteries by putting together (10)-(11). The model state is $\mathrm{SoC}_k$ and the parameters are $K_i$ for $i = 0, \cdots, 3$ and $R$.

For adaptive SoC estimation, we will perform simultaneous estimation of the SoC and the parameters. To obtain a locally observable model, one or several parameters usually need to be fixed in order to estimate the others and the SoC. A few options may exist regarding which parameters are fixed. Based on our experience with the considered model, we separate the parameters into two sets, fix one set and augment the state vector to incorporate the SoC and the other set. Accordingly, two submodels will be constructed.

Letting $K_0$ and $K_1$ be fixed, the first one can be obtained:

$$\mathscr{M}_1 : \begin{cases} \mathbf{x}_{k+1}^1 = \mathbf{f}^1(\mathbf{x}_k^1, u_k), \\ y_k = h^1(\mathbf{x}_k^1, u_k), \end{cases} \tag{12}$$

where

$$\begin{aligned} \mathbf{x}_k^1 &= \begin{bmatrix} \mathrm{SoC}_k & K_2 & K_3 & R \end{bmatrix}^\top, \\ \mathbf{f}_1(\mathbf{x}_k^1, u_k) &= \mathbf{x}_k^1 - \begin{bmatrix} K_0 & 0 & 0 & 0 \end{bmatrix}^\top u_k, \\ h_1(\mathbf{x}_k^1, u_k) &= K_1 + \mathbf{x}_{k,2}^1 \ln(\tau_1 + \mathbf{x}_{k,1}^1) + \mathbf{x}_{k,3}^1 \ln(\tau_2 + 1 - \mathbf{x}_{k,1}^1) - \mathbf{x}_{k,4}^1 u_k. \end{aligned}$$

Analogously, by fixing $K_i$ for $i = 1, 2, 3$, we have

$$\mathscr{M}_2 : \begin{cases} \mathbf{x}_{k+1}^2 = \mathbf{f}^2(\mathbf{x}_k^2, u_k), \\ y_k = h^2(\mathbf{x}_k^2, u_k), \end{cases} \tag{13}$$

where

$$\begin{aligned} \mathbf{x}_k^2 &= \begin{bmatrix} \mathrm{SoC}_k & K_0 & R \end{bmatrix}^\top, \\ \mathbf{f}^2(\mathbf{x}_k^2, u_k) &= \begin{bmatrix} \mathbf{x}_{k,1}^2 - \mathbf{x}_{k,2}^2 u_k & 0 & 0 \end{bmatrix}^\top, \\ h^2(\mathbf{x}_k^2, u_k) &= K_1 + K_2 \ln(\tau_1 + \mathbf{x}_{k,1}^2) + K_3 \ln(\tau_2 + 1 - \mathbf{x}_{k,1}^2) - \mathbf{x}_{k,3}^2 u_k. \end{aligned}$$

**Remark 1.** In an implicit manner, $\mathscr{M}_1$ places more confidence on the state equation (11), assuming that $K_0$ is accurate, while the belief in the measurement equation (10) is emphasized in $\mathscr{M}_2$ similarly. Nevertheless, it is noteworthy that the confidence level on each submodel during the estimation process is dynamically determined by the fusion strategy outlined earlier in Section 2.

**Remark 2.** An extended series can be constructed on the basis of each submodel if we let the parameters take different values that are believed to be close or equal to the truth. For instance, the Coulombic efficiency may be 100%, 90% or even 80% depending on the operating conditions. Then $\mathscr{M}_1$ will give birth to three more submodels if $K_0$ assumes $\Delta T/C_0$, $0.9\Delta T/C_0$ and $0.8\Delta T/C_0$, respectively. This allows considerable flexibility for us to describe the battery dynamics and brings improvements to the single-model case.

### *3.2. Observability Analysis*

It is well-known that state estimation requires a 'certain' kind of observability of the system. Hence, we will analyze the observability properties of $\mathscr{M}_1$ and $\mathscr{M}_2$ before proceeding to SoC estimation.

Consider a general single-input-single-output (SISO) system

$$\mathscr{S}: \begin{cases} \mathbf{x}_{k+1} = \mathbf{f}(\mathbf{x}_k, u_k), \\ \quad y_k = h(\mathbf{x}_k, u_k), \end{cases} \tag{14}$$

where $\mathbf{x} \in \mathbb{X}$ of dimension $n$, $y \in \mathbb{Y}$ and $u \in \mathbb{U}$. We assume that 1) $\mathbb{X}$ and $\mathbb{Y}$ connected, second countable, Hausdorff, differentiable manifolds of class $C^q$ with $q \in \mathbb{N}$, 2) $\mathbb{U}$ is an open interval of $\mathbb{R}$, and 3) $\mathbf{f}: \mathbb{X} \times \mathbb{U} \to \mathbb{X}$ and $h: \mathbb{X} \to \mathbb{Y}$ are of class $C^q$. For convenience, $\mathbf{f}(\mathbf{x}, u)$ is denoted as $\mathbf{f}^u(\mathbf{x})$, and $h(\mathbf{f}(\mathbf{x}, u_0), u_1) = h^{u_1} \circ \mathbf{f}^{u_0}(\mathbf{x})$. Following [23, 24], the local observability for $\mathscr{S}$ is defined as follows:

**Definition 1.** (Distinguishability) *Two states $\mathbf{x}$ and $\mathbf{x}^*$ are said to be indistinguishable, written as $\mathbf{x} \rightleftarrows \mathbf{x}^*$, if for each $l \neq 0$ and for each input sequence, $\{u_0, \cdots, u_l\} \in \mathbb{U}^l$, we have*

$$h^{u_l} \circ \mathbf{f}^{u_{l-1}} \circ \cdots \circ \mathbf{f}^{u_0}(\mathbf{x}) = h^{u_l} \circ \mathbf{f}^{u_{l-1}} \cdots \circ \mathbf{f}^{\mathbf{u}_0}(\mathbf{x}^*).$$

*Otherwise, they are distinguishable.*

**Definition 2.** (Local observability) *The system $\mathscr{S}$ is locally observable if for any state $\mathbf{x}^o \in \mathbb{X}$, there exists a neighborhood $\mathbb{D}$ of $\mathbf{x}^o$ such that, $\mathbf{x} \rightleftarrows \mathbf{x}^*$ implies $\mathbf{x} = \mathbf{x}^*$ for each $\mathbf{x}, \mathbf{x}^* \in \mathbb{D}$.*

By Definitions 1-2, local observability means that $\mathbf{x}^o$ can be distinguished from its neighbors given the input sequence $\{u_0, \cdots, u_l\}$ and the output sequence $y_0, \cdots, y_l$. It should be noted that this definition of observability depends not only on the system itself but also on the applied inputs, unlike the uniform observability for any inputs defined in [25]. While one sees various definitions of nonlinear observability in the literature, this does not obstruct our discussion since they are usually about 'different measurements results from different initial states (for admissible inputs)'. The interested reader can refer to the literature on the subject, e.g., [26].

To address the observability condition, the following sets of functions are defined:

$$
\begin{aligned}
\Omega_0 &= \{h(\cdot)\},\\
\Omega_l &= \{h^{u_j} \circ \mathbf{f}^{u_{j-1}} \circ \cdots \circ \mathbf{f}^{u_0}(\cdot) : u_i \in \mathbb{U} \forall i = 1, \cdots, j \text{ and } 1 \leq j \leq l\},\\
\Omega &= \cup_{j\geq 0}\Omega_l.
\end{aligned}
$$

An observability criterion is presented in the following theorem, please see [23] for the proof.

**Theorem 1.** *[23] If* $\dim \mathrm{d}\Omega(\mathbf{x}) = n\ \forall \mathbf{x} \in \mathbb{X}$*, then the system* $\mathscr{S}$ *is locally observable.*

Theorem 1 gives a sufficient condition to determine the local observability by relating it to the full dimensionality of the codistribution $\mathrm{d}\Omega$. Now the local observability of $\mathscr{M}_1$ and $\mathscr{M}_2$ can be analyzed using Theorem 1. Let us take $\mathscr{M}_1$ for an example since the analysis for both follows similar lines.

Note that $\mathbf{f}^1$ and $h^1$ are of class $C^\infty$. Suppose that the initial state is $\mathbf{x}_0^1$ for $\mathscr{M}_1$ and that there are $L$ measurements $\{y_1, \cdots, y_L\}$. By (12), $\mathbf{x}_k^1$ is given by

$$
\mathbf{x}_k^1 = \mathbf{x}_0^1 - \begin{bmatrix} K_0 & 0 & 0 & 0 \end{bmatrix}^\top \sum_{i=0}^{k-1} u_i.
$$

Hence, we have

$$
\begin{aligned}
\bar{h}_k^1(\mathbf{x}_0^1) &= h^{1u_k} \circ \mathbf{f}^{1u_{k-1}} \circ \cdots \circ \mathbf{f}^{1u_0}(\mathbf{x}_0^1)\\
&= K_1 + \mathbf{x}_{0,2}^1 \ln\left(\tau_1 + \mathbf{x}_{0,1}^1 - K_0 \sum_{i=0}^{k-1} u_i\right) + \mathbf{x}_{0,3}^1 \ln\left(\tau_2 + 1 - \mathbf{x}_{0,1}^1 + K_0 \sum_{i=0}^{k-1} u_i\right) - \mathbf{x}_{0,4}^1 u_k,
\end{aligned}
$$

where $\bar{h}_k^1 \in \Omega$. Define a matrix $\mathbf{J}$ with dimensions $L \times 4$:

$$
\mathbf{J} = \begin{bmatrix} \frac{\mathrm{d}\bar{h}_1^1}{\mathrm{d}\mathbf{x}_0^1} & \cdots & \frac{\mathrm{d}\bar{h}_k^1}{\mathrm{d}\mathbf{x}_0^1} & \cdots & \frac{\mathrm{d}\bar{h}_L^1}{\mathrm{d}\mathbf{x}_0^1} \end{bmatrix}^\top .
$$

The elements in the $k$-th row of $\mathbf{J}$ are

$$
\mathbf{J}_{k,1} = \frac{\partial \bar{h}_k^1}{\partial \mathbf{x}_{0,1}^1} = \frac{\mathbf{x}_{0,2}^1}{\tau_1 + \mathbf{x}_{0,1}^1 - K_0 \sum_{i=0}^{k-1} u_i} - \frac{\mathbf{x}_{0,3}^1}{\tau_2 + 1 - \mathbf{x}_{0,1}^1 + K_0 \sum_{i=0}^{k-1} u_i},
$$

$$\mathbf{J}_{k,2} = \frac{\partial \bar{h}_k^1}{\partial \mathbf{x}_{0,2}^1} = \ln\left(\tau_1 + \mathbf{x}_{0,1}^1 - K_0 \sum_{i=0}^{k-1} u_i\right),$$
$$\mathbf{J}_{k,3} = \frac{\partial \bar{h}_k^1}{\partial \mathbf{x}_{0,3}^1} = \ln\left(\tau_2 + 1 - \mathbf{x}_{0,1}^1 + K_0 \sum_{i=0}^{k-1} u_i\right),$$
$$\mathbf{J}_{k,4} = \frac{\partial \bar{h}_k^1}{\partial \mathbf{x}_{0,4}^1} = -u_k.$$

By observation, we have the following conclusions:

- The submodel $\mathscr{M}_1$ is locally observable if a suitable input sequence $\{u_k\}$ is applied. By 'suitable', we mean that $u_k$ varies sufficiently in magnitude over time, or in other words, $\{u_k\}$ contains a rich mix of frequency contents. In this case, $\mathbf{J}$ will have full column rank, and as a result, dim d$\Omega$ has a dimension of 4, satisfying the condition in Theorem 1. It should be emphasized such a condition imposed on the input is a mild constraint that can be easily satisfied when a battery is in use.

- We can analogously determine that $\mathscr{M}_2$ is also locally observable if a suitable $\{u_k\}$ is used to excite the system.

- Additional submodels other than $\mathscr{M}_1$ and $\mathscr{M}_2$ can be constructed by fixing different parameters. An example is to fix only $K_1$, which will lead to another locally observable model. However, no matter how many submodels are used, the essence of multi-model adaptive SoC estimation remains the same, as will be seen in Section 4. It is also noteworthy that the resultant submodel will be unobservable if all the parameters are assumed unknown.

## 4. Multi-model Adaptive SoC Estimation

In this section, we study multi-model adaptive SoC estimation on the basis of Sections 2 and 3. An IEKF-based elemental filter will be applied to $\mathscr{M}_1$ and $\mathscr{M}_2$, respectively, for adaptive SoC estimation. The overall estimate will be obtained by fusing all the estimates for the elemental filters, leading to the `MM-AdaSoC` algorithm.

### 4.1. Adaptive SoC Estimation

Adaptive SoC estimation can be attained via state estimation, because the state vector of each consists of both the SoC variable and the parameters. Following [13], we use the IEKF. As an improved version of the EKF, it is capable of giving more accurate state estimates even for highly nonlinear systems by iteratively refining the estimate around the current point at each time instant.

Consider applying the IEKF to the system in (14). At $k-1$, prediction can be made about the next time instant. The formulas are as follows:

$$\hat{\mathbf{x}}_{k|k-1} = \mathbf{f}(\hat{\mathbf{x}}_{k-1|k-1}, u_{k-1}), \tag{15}$$

$$\mathbf{P}_{k|k-1} = \mathbf{F}_{k-1}\mathbf{P}_{k-1|k-1}\mathbf{F}_{k-1}^{\top} + \mathbf{Q}, \tag{16}$$

where $\hat{\mathbf{x}}$ is the estimate of $\mathbf{x}$, $\mathbf{P}$ is the error covariance, $\mathbf{Q} \geq 0$ is an adjustable matrix to account for the process noise, and $\mathbf{F}$ is given by

$$\mathbf{F}_{k-1} = \frac{\partial \mathbf{f}}{\partial \mathbf{x}} \left(\hat{\mathbf{x}}_{k-1|k-1}, u_{k-1}\right).$$

When the measurement $y_k$ arrives, $\hat{\mathbf{x}}_{k|k-1}$ can be updated by the new information $y_k$ brings. The procedure is based on iteration. Let $\ell$ denote the iteration number and $\hat{\mathbf{x}}_{k|k}^{(\ell)} = \hat{\mathbf{x}}_{k|k-1}$ for $\ell = 0$. The update formulas are

$$\mathbf{K}_k^{(\ell)} = \mathbf{P}_{k|k-1}\mathbf{H}_k^{(\ell-1)} \left[\mathbf{H}_k^{(\ell-1)}\mathbf{P}_{k|k-1}\mathbf{H}_k^{(\ell-1)^{\top}} + R\right]^{-1}, \tag{17}$$

$$\hat{y}_k^{(\ell)} = h\left(\hat{\mathbf{x}}_{k|k}^{(\ell-1)}, u_k\right), \tag{18}$$

$$\hat{\mathbf{x}}_{k|k}^{(\ell)} = \hat{\mathbf{x}}_{k|k-1} + \mathbf{K}_k^{(\ell)} \left[y_k - \hat{y}_k^{(\ell)} - \mathbf{H}_k^{(\ell-1)} \left(\hat{\mathbf{x}}_{k|k-1} - \hat{\mathbf{x}}_{k|k}^{(\ell-1)}\right)\right], \tag{19}$$

where $R > 0$ accounts for the measurement noise and

$$\mathbf{H}_k^{(\ell)} = \frac{\partial h}{\partial \mathbf{x}} \left(\hat{\mathbf{x}}_{k|k}^{(\ell)}, u_k\right).$$

The iteration process stops when $\ell$ achieves the pre-specified maximum iteration number $\ell_{\max}$ or when the error between two consecutive iterations is less than the pre-selected tolerance level. Then $\hat{\mathbf{x}}_{k|k} = \hat{\mathbf{x}}_{k|k}^{(\ell_{\max})}$, and the associated error covariance is given by

$$\mathbf{P}_{k|k} = \left[\mathbf{I} - \mathbf{K}_k^{(\ell_{\max})}\mathbf{H}_k^{(\ell_{\max})}\right]\mathbf{P}_{k|k-1}.$$

Following the above description, the IEKF can be applied as an elemental filter to $\mathscr{M}_1$ and $\mathscr{M}_2$. The resultant state estimates are $\hat{\mathbf{x}}_{k|k}^1$ and $\hat{\mathbf{x}}_{k|k}^2$, respectively. Accordingly, the SoC estimates are denoted as $\widehat{\mathrm{SoC}}_k^1 = \hat{\mathbf{x}}_{k|k,1}^1$ and $\widehat{\mathrm{SoC}}_k^2 = \hat{\mathbf{x}}_{k|k,1}^2$, respectively.

### 4.2. `MM-AdaSoC`: Multi-model Adaptive SoC Estimation

The SoC estimates produced from $\mathscr{M}_1$ and $\mathscr{M}_2$, $\widehat{\mathrm{SoC}}_k^1$ and $\widehat{\mathrm{SoC}}_k^2$, respectively, can be combined weightedly to generate the overall estimate $\widehat{\mathrm{SoC}}_k$. In the light of the fusion strategy in (7)-(8), we have

$$\widehat{\mathrm{SoC}}_k = \sum_{i=1}^{2} \widehat{\mathrm{SoC}}_k^i \mu_i, \tag{20}$$

where the weight coefficient $\mu_i$ for $i = 1, 2$ can be determined using (6).

Putting together the results, we obtain the `MM-AdaSoC` algorithm, as is summarized in Table 1.

**Remark 3.** The underlying idea of the proposed `MM-AdaSoC` algorithm is that the IEKF-based adaptive SoC estimation is carried out for multiple models and then the estimation results are fused to yield the overall SoC estimate. For the `MM-AdaSoC`, the recursive and real-time implementation cuts down the amount of stored data. Meanwhile, higher estimation accuracy is achieved, because the update procedure relies on iterative searching at each recursion. Another noteworthy advantage is that a good balance is maintained between the estimation performance and the computational complexity, conceding a generally linear moderate increase of the demanded computing power depending on the number of models used.

**Remark 4.** The applicability of the proposed `MM-AdaSoC` algorithm to different types of batteries is quite promising. Due to its parameterized characterization, the Nernst model has been found capable of describing the dynamics of many batteries, e.g., nickel metal hydride (NiMH), $LiMn_2O_4$ and $LiCoO_2$. As a result, the `MM-AdaSoC` algorithm can be well applied to such batteries for its construction based on the Nernst model.

**Remark 5.** Not limited to the `MM-AdaSoC` algorithm at all, the role that multi-model estimation can play is more profound. It can be developed as a framework, within which variety of advanced estimation methods can be built for battery applications. Here, we identify five potential sources of multiple models:

- a set of submodels established from a battery model by fixing certain parameters for adaptive SoC estimation, as we have done in this paper,
- a set of submodels established from a model by assuming different sets of values for model parameters,

- a set of different models constructed in different ways, such as an equivalent-circuit model and an electrochemical-principles-based model,
- a set of models capturing different characteristics of batteries, e.g., the charging and discharging processes, cycling and aging effects, and
- a multitude of (sub)models combining the above four cases.

The multi-model approach promises three-fold benefits.

- It better apprehends the battery dynamics known to be complex and multi-faceted, thus promoting the accuracy and robustness of SoC estimation.
- It reduces the complexity of estimator design, especially when highly nonlinear battery dynamics are involved, in a 'divide-and-conquer' manner. Simple and elegant solutions will be achieved and theoretical analysis is made easier.
- It can even provide useful model interpretation and comparison in some circumstances. We note that research on relevant topics would be of much interest and requires further exploration.

To fully realize its potential and benefits, multi-model estimation/control for batteries needs to be further studied in the future.

## 5. Application Examples

In this section, we present two examples using simulation and experiment data, respectively, to evaluate the `MM-AdaSoC` algorithm.

**Example 1.** This example is based on simulation with a model used in [15] for a NiMH battery system. For simulation purpose, we employ certain minor modification, but the obtained model is still considered to be a sufficiently accurate representation of the NiMH battery dynamics in most circumstances. The change of SoC is governed by

$$\mathrm{SoC}_{k+1} = \mathrm{SoC}_k - \frac{\eta \cdot \Delta T}{C_0} u_k - \frac{S_D(T_{\mathrm{ref}}) \cdot \Delta T}{100},$$

where the third term on the right-hand side represents self-discharge with

$$S_D(T_{\mathrm{ref}}) = k_0 \exp\left( -\frac{E_{A,S}}{R_g T_{\mathrm{ref}}} \right) \mathrm{SoC}.$$

Here, $k_0 = 1.0683 \times 10^7$ per hour, $E_{A,S}/R_g = 6,789$K, the current efficiency $\eta = 1$ for discharging and 0.99 for charging near 50% SoC, the nominal capacity $C_0 = 1.25$Ah, the reference temperature $T = 35°$C (308.15K), and the sampling period $\Delta T = 1$s. The initial SoC is assumed to be 50%. The terminal voltage is equal to the OCV plus internal-resistance-induced drop, that is,

$$y_k = V_{oc,k} - \bar{R}u_k.$$

The OCV $V_{oc}$ is given by the following equation with the inclusion of voltage hysteresis:

$$V_{oc} = U_0 + \frac{R_g T_{\text{ref}}}{n_e F} \ln\left(\frac{\text{SoC}_k - \Pi}{1 - \text{SoC}_k}\right) + V_{H,k},$$

where the varying voltage hysteresis $V_H$ is characterized by an empirical expression

$$V_{H,k+1} = V_{H,k} - \beta \cdot \eta \cdot \left[V_{H,\max} + \text{sign}(u_k) \cdot V_{H,k}\right] \cdot \Delta T \cdot u_k.$$

The resistance $\bar{R}$ is described by

$$\bar{R} = \sum_{j=0}^{n} a_j \text{SoC}^j.$$

The Farady's constant $F = 96,487$C mol$^{-1}$, $n_e = 1$, $R_g = 8.314$J mol$^{-1}$ K$^{-1}$, $U_0 = 1.37$V, $\Pi = 0.08$, $\beta = 3 \times 10^{-5}$C$^{-1}$, $V_{H,\max} = 0.05$V. The initial $V_H$ is 0.005V. In addition, $a_0 = 4.1252 \times 10^{-2}$, $a_1 = 8.9691 \times 10^{-4}$, $a_2 = 1.6760 \times 10^{-5}$, $a_3 = -1.4435 \times 10^{-7}$ and $a_4 = 4.7223 \times 10^{-10}$.

During the simulation, we do not assume that this model is fully available for SoC estimation. Instead, the modified Nernst model presented in Section 3 will be used for approximate description of the above true model. Let $K_0 = \eta \cdot \Delta T / C_0$, $K_1 = U_0$, $K_2 = K_3 = R_g T_{\text{ref}} / (n_e F)$, $\tau_1 = -\Pi$, $\tau_2 = 0$ and $R = a_0$. The current signal applied as the input to the battery was a pseudo-random binary sequence (PRBS) stretched by 100 times over the time axis. Its magnitude is 1A. A view of the input current and output voltage during the first 2000 time instants is given in Fig. 3(a). Let the true initial SoC be 55% and the initial SoC estimate be 65%. The initial weights assigned to $\mathscr{M}_1$ and $\mathscr{M}_2$ are 0.7 and 0.3, respectively.

In this setting, we face hysteresis, model mismatch and incorrect initial estimate, which together make SoC estimation a tougher challenge. As described in previous sections, we consider two submodels, with the first one assuming known $K_0$ and $K_1$ and the second assuming known $K_1$, $K_2$ and $K_3$. When the `MM-AdaSoC` algorithm is applied, Fig. 3(b) shows the estimation of the SoC over time. We see that both $\mathscr{M}_1$- and $\mathscr{M}_2$-based estimates differ from the actual values with bounded errors. However, it turns out that the overall estimates given by the MM-AdaSoC algorithm become more accurate, demonstrating that the estimation errors can be reduced effectively by fusion of the multi-model estimates. The weights of the two models are compared in Fig. 3(c). Obviously, $\mathscr{M}_2$ weighs much more than $\mathscr{M}_1$ in this case. This is because $\mathscr{M}_1$ is sensitive to the initial SoC estimate, relying on the state equation based on Coulomb counting. Furthermore, we also apply the well-known EKF to the modified Nernst model with known $K_i$ for $i = 0, 1, 2, 3$ for SoC estimation. As shown in Fig. 3(d), the EKF yields unreliable results in this situation in comparison to the MM-AdaSoC algorithm.

**Example 2.** For the experimental evaluation of the MM-AdaSoC algorithm, data was collected from a $LiMn_2O_4$/hard-carbon battery in the Advanced Technology R&D Center, Mitsubishi Electric Corporation. The experiment was conducted using a rechargeable battery test equipment produced by Fujitsu Telecom Networks. The current input was a PRBS signal stretched by 10 times over the time axis with a magnitude of 5A. Despite many other options, we chose the PRBS because it has white-noise-like properties and is admissible for observability. The profile of the input current and the output voltage is shown in Fig. 4. The battery has a nominal capacity of 4.93Ah. The sampling period was 1s. During the experiment, the ambient temperature in the chamber was maintained at 25.8°C.

We consider the model in (10)-(11). The Coulombic efficiency constant $K_0 = 5.6342 \times 10^{-5}$ when $u_k > 0$ (100% for discharging) and $K_0 = 4.7891 \times 10^{-5}$ when $u_k < 0$ (85% for charging). From the SoC-OCV data collected from this type of batteries, it can be determined that $K_1 = 1.294$, $K_2 = 0.0984$, $K_3 = 3.972$, $\tau_1 = \tau_2 = 0.3$.

As aforementioned, the actual values of the parameters $K_i$ for $i = 0, \cdots, 3$ can change as a result of the operating conditions. Hence, rather than depending fully on their nominal values, we perform multi-model adaptive SoC estimation by applying the MM-AdaSoC algorithm. The construction of two submodels from (10)-(11) is described in Section 3.1.

The SoC estimation results are shown in Fig. 5. The full view over the available experimental data is given in Fig. 5(a). The initial SoC of the battery is known to be approximately 50%. It is seen that there is a difference of approximately 5% between the $\mathscr{M}_1$-based and $\mathscr{M}_2$-based estimates. Based on our experience, $\mathscr{M}_1$ tends to yield conservative estimates in this case and $\mathscr{M}_2$ does the opposite. The MM-AdaSoC algorithm, through the fusion strategy, makes adjustment to give neutralized overall estimates. Although the true SoC data are not available, we still judge that the estimates are close to the truth, based on our *a priori* knowledge about the battery behavior. Fig. 5(b) illustrates what happens during the initial 450s. It is seen from Figs. 5(a)-5(b) that the overall estimates are closer to those based on $\mathscr{M}_2$. This is verified in Figs. 5(c)-5(d), where the weight $\mu_1$ for $\mathscr{M}_1$ fluctuates slightly around 0.63 and $\mu_2$ around 0.37. Thus, with a larger weight, $\mathscr{M}_1$ is given more confidence than $\mathscr{M}_2$ by the `MM-AdaSoC` algorithm during the implementation. It is understood that the fusion depends on the performance of one-step-forward prediction of the terminal voltage. Fig. 5(e) compares the measured data with the prediction based on $\mathscr{M}_1$ and $\mathscr{M}_2$, respectively. The prediction is satisfactory for both submodels, but $\mathscr{M}_2$ is observed to lead to the better predicted voltage.

From the above results, we believe that the `MM-AdaSoC` algorithm is quite effective, supported by the findings that the obtained SoC estimates exhibit considerable accuracy and that the voltage prediction approximates the truth well. Through experiments with charging/discharging rates of 0.5A, 1A, 10A and 15A, we consistently observe similar estimation results, which shows that the applicability of the model and the power of the `MM-AdaSoC` algorithm.

## 6. Conclusions

Development of adaptive approaches for SoC estimation is of practical significance, because battery dynamics are often hard to fully determine and are time-varying. We are focused on improving the adaptive SoC estimation via launching a multi-model strategy in this paper, motivated by the proven success of multi-model estimation in addressing problems involving structural and parameter changes.

The main contribution of this paper is the development and validation of the `MM-AdaSoC` algorithm. It is built to estimate a battery's SoC in real time through carrying out simultaneous state and parameter estimation on a set of (sub)models. We first construct two submodels from a general state-space battery model by fixing different parameters, with both shown to be locally observable with admissible inputs. The well-known IEKF is then applied to each submodel to produce the SoC and parameter estimates. The final overall estimates are generated by fusing the submodel-based estimates, and it is shown that the fusion is a linear weighted combination of the estimates. Simulation and experimental results are presented to demonstrate and validate the effectiveness of the algorithm.

Apart from the `MM-AdaSoC` algorithm, we also emphasize the potential of the multi-model framework for battery applications. The initial success reported in this paper would provide strong incentives for further development of a wide range of methods based on multiple models to better monitor the status and health of a battery.

## Acknowledgement

The authors would like to thank Prof. Scott Moura for his valuable and constructive suggestions that led to the improvement of this paper.



[1] N. Chaturvedi, R. Klein, J. Christensen, J. Ahmed, A. Kojic, Algorithms for Advanced Battery-Management Systems, IEEE Control Systems Magazine 30 (3) (2010) 49–68.

[2] V. Pop, H. J. Bergveld, P. H. L. Notten, P. P. L. Regtien, State-of-the-art of battery state-of-charge determination, Measurement Science and Technology 16 (12) (2005) R93–110.

[3] R. Rao, S. Vrudhula, D. Rakhmatov, Battery modeling for energy aware system design, Computer 36 (12) (2003) 77–87.

[4] S. Santhanagopalan, R. E. White, Online estimation of the state of charge of a lithium ion cell, Journal of Power Sources 161 (2) (2006) 1346–55.

[5] G. L. Plett, Extended Kalman filtering for battery management systems of LiPB-based HEV battery packs: Part 3. State and parameter estimation, Journal of Power Sources 134 (2) (2004) 277–92.

[6] D. Domenico, G. Di Fiengo, A. Stefanopoulou, Lithium-ion battery state of charge estimation with a Kalman filter based on a electrochemical model, in: Proc. IEEE International Conference on Control Applications, 702–7, 2008.

[7] J. Lee, O. Nam, B. Cho, Li-ion battery SOC estimation method based on the reduced order extended Kalman filtering, Journal of Power Sources 174 (1) (2007) 9–15.

[8] J. Han, D. Kim, M. Sunwoo, State-of-charge estimation of lead-acid batteries using an adaptive extended Kalman filter, Journal of Power Sources 188 (2) (2009) 606–12.

[9] O. Barbarisi, F. Vasca, L. Glielmo, State of charge Kalman filter estimator for automotive batteries, Control Engineering Practice 14 (3) (2006) 267–75.

[10] K. Smith, C. Rahn, C.-Y. Wang, Model-Based Electrochemical Estimation and Constraint Management for Pulse Operation of Lithium Ion Batteries, IEEE Transactions on Control Systems Technology 18 (3) (2010) 654–63, ISSN 1063-6536.

[11] G. L. Plett, Sigma-point Kalman filtering for battery management systems of LiPB-based HEV battery packs: Part 2: Simultaneous state and parameter estimation, Journal of Power Sources 161 (2) (2006) 1369–84.

[12] S. Santhanagopalan, R. E. White, State of charge estimation using an unscented filter for high power lithium ion cells, International Journal of Energy Research 34 (2) (2010) 152–63.

[13] H. Fang, Y. Wang, Z. Sahinoglu, T. Wada, S. Hara, Adaptive Estimation of State of Charge for Lithium-ion Batteries, in: Proc. American Control Conference, 3485–91, 2013.

[14] I.-S. Kim, The novel state of charge estimation method for lithium battery using sliding mode observer, Journal of Power Sources 163 (1) (2006) 584–90.

[15] M. Verbrugge, E. Tate, Adaptive state of charge algorithm for nickel metal hydride batteries including hysteresis phenomena, Journal of Power Sources 126 (1-2) (2004) 236–49.

[16] Y. Hu, S. Yurkovich, Battery cell state-of-charge estimation using linear parameter varying system techniques, Journal of Power Sources 198 (2012) 338–50.

[17] R. Klein, N. Chaturvedi, J. Christensen, J. Ahmed, R. Findeisen, A. Kojic, Electrochemical Model Based Observer Design for a Lithium-Ion Battery, IEEE Transactions on Control Systems Technology 21 (2) (2013) 289–301.

[18] S. J. Moura, N. A. Chaturvedi, M. Krstic, PDE Estimation Techniques for Advanced Battery Management Systems - Part I: SOC Estimation, in: Proc. American Control Conference, 559–65, 2012.

[19] S. J. Moura, N. A. Chaturvedi, M. Krstic, Adaptive PDE Observer for Battery SOC/SOH Estimation via an Electrochemical Model, ASME Journal of Dynamic Systems, Measurement, and Control .

[20] P. S. Maybeck, Stochastic Models, Estimation, and Control Volume 2, Academic Press, New York, 1982.

[21] D. Simon, Optimal State Estimation: Kalman, $\mathscr{H}_\infty$, and Nonlinear Approaches, John Wiley & Sons, 2006.

[22] X. Li, V. Jilkov, Survey of maneuvering target tracking. Part V: Multiple-model methods, IEEE Transactions on Aerospace and Electronic Systems 41 (4) (2005) 1255–321.

[23] F. Albertini, D. D'Alessandro, Observability and Forward-Backward Observability of Discrete-Time Nonlinear Systems, Mathematics of Control, Signals and Systems 15 (4) (2002) 275–90.

[24] H. Nijmeijer, A. van der Schaft, Nonlinear Dynamical Control Systems, Springer, 1990.

[25] J.-P. Gauthier, H. Hammouri, S. Othman, A simple observer for nonlinear systems applications to bioreactors, IEEE Transactions on Automatic Control 37 (6) (1992) 875–80.

[26] R. Hermann, A. J. Krener, Nonlinear controllability and observability, IEEE Transactions on Automatic Control 22 (5) (1977) 728–40.

## List of Tables


1 The `MM-AdaSoC` algorithm: Adaptive SoC estimation using multiple models. . . 22

## List of Figures


1 A schematic description of adaptive SoC estimation. . . . . . . . . . . . . . . . . 23

2 The structure of a multi-model estimator. . . . . . . . . . . . . . . . . . . . . . . . 23

3 (a) The input current-output voltage profile; (b) SoC estimates versus truth over time; (c) fusion weights for $\mathscr{M}_1$ and $\mathscr{M}_2$ versus time; (d) comparison with the EKF. 24

4 The input-output (current-voltage) profile. . . . . . . . . . . . . . . . . . . . . . . 24

5 (a) SoC estimates versus time; (b) SoC estimates during the initial 450s; (c) fusion weights for $\mathscr{M}_1$ and $\mathscr{M}_2$ versus time; (d) fusion weights during the initial 450s; (e) comparison between the true and the one-step-forward predicted voltage. . . . . 25

initialize the implementation: $k=0$, $\hat{\mathbf{x}}^i_{0|0}=\mathbf{x}^i_0$, $\mathbf{P}^i_{0|0}=\delta^i\mathbf{I}$, where $\delta^i \gg 0$, for $i=1,2$

**repeat**

$k \leftarrow k+1$

*IEKF based adaptive SoC estimation:*

**for** $i=1$ to 2 **do**

import the submodel $\mathscr{M}_i$

*$\mathscr{M}_i$-based prediction (time-update):*

project the state ahead to obtain $\hat{\mathbf{x}}^i_{k|k-1}$

$$\hat{\mathbf{x}}^i_{k|k-1}=\mathbf{f}^i(\hat{\mathbf{x}}^i_{k-1|k-1},u_{k-1})$$

project the error covariance ahead to obtain $\mathbf{P}^i_{k|k-1}$

$$\mathbf{F}^i_{k-1}=\frac{\partial \mathbf{f}^i}{\partial \mathbf{x}^i}\left(\hat{\mathbf{x}}^i_{k-1|k-1},u_k\right),\ \ \mathbf{P}^i_{k|k-1}=\mathbf{F}^i_{k-1}\mathbf{P}^i_{k-1|k-1}\mathbf{F}^{i\,\top}_{k-1}+\mathbf{Q}^i$$

*$\mathscr{M}_i$-based update (measurement-update):*

initialize the iteration procedure: $\ell=0$, $\hat{\mathbf{x}}^{i(0)}_{k|k}=\hat{\mathbf{x}}^i_{k|k-1}$

**while** $\ell<\ell_{\max}$ **do**

$\ell \leftarrow \ell+1$

compute the Kalman gain matrix

$$\mathbf{H}^{i(\ell)}_k=\frac{\partial h^i}{\partial \mathbf{x}^i}\left(\hat{\mathbf{x}}^{i(\ell)}_{k|k},u_k\right),\ \ \mathbf{K}^{i(\ell)}_k=\mathbf{P}^i_{k|k-1}\mathbf{H}^{i(\ell-1)}_k\left[\mathbf{H}^{i(\ell-1)}_k\mathbf{P}^i_{k|k-1}\mathbf{H}^{i(\ell-1)\,\top}_k+R^i\right]^{-1}$$

update the state estimate

$$\hat{\mathbf{x}}^{i(\ell)}_{k|k}=\hat{\mathbf{x}}^i_{k|k-1}+\mathbf{K}^{(\ell)}_k\left[y_k-h^i\left(\hat{\mathbf{x}}^{i(\ell-1)}_{k|k},u_k\right)-\mathbf{H}^{(\ell-1)}_k\left(\hat{\mathbf{x}}^i_{k|k-1}-\hat{\mathbf{x}}^{i(\ell-1)}_{k|k}\right)\right]$$

**end while**

assign $\hat{\mathbf{x}}^i_{k|k}=\hat{\mathbf{x}}^{i(\ell_{\max})}_{k|k}$

update the error covariance

$$\mathbf{P}_{k|k}=\left[\mathbf{I}-\mathbf{K}^{(\ell_{\max})}_k\mathbf{H}^{(\ell_{\max})}_k\right]\mathbf{P}_{k|k-1}$$

export $\mathscr{M}_i$-based SoC estimate $\widehat{\mathrm{SoC}}^i_k=\hat{\mathbf{x}}^i_{k|k,1}$

**end for**

*Estimation fusion*

determine the probability $\pi^i_k$ that the battery runs on $\mathscr{M}_i$ for $i=1,2$ with $\sum_{i=1}^2\pi^i_k=1$

**for** $i=1$ to 2 **do**

compute the initial weights

$$\mathbf{H}^i_k=\frac{\partial h^i}{\partial \mathbf{x}^i}\left(\hat{\mathbf{x}}^i_{k|k-1},u_k\right),\ \ S^i_k=\mathbf{H}^i_k\mathbf{P}^i_{k|k-1}(\mathbf{H}^i_k)^\top+R^i$$

$$\hat{y}^i_{k|k-1}=h^i(\hat{\mathbf{x}}^i_{k|k-1},u_k),\ \ \tilde{y}^i_{k|k-1}=y_k-\hat{y}^i_{k|k-1},\ \ w^i_k=(2\pi)^{-\frac{n}{2}}(S^i_k)^{-\frac{1}{2}}\exp\left[-\frac{(\tilde{y}^i_k)^2}{2S^i_k}\right]$$

**end for**

compute the normalized weights

$$\mu^i_k=\frac{w^i_k\pi^i_k}{\sum_{j=1}^N w^j_k\pi^j_k}\ \text{for}\ i=1,2$$

fuse the SoC estimates from $\mathscr{M}_1$ and $\mathscr{M}_2$

$$\widehat{\mathrm{SoC}}_k=\sum_{i=1}^2\widehat{\mathrm{SoC}}^i_k\mu_i$$

**until** SoC estimation task ends

Table 1: The `MM-AdaSoC` algorithm: Adaptive SoC estimation using multiple models.

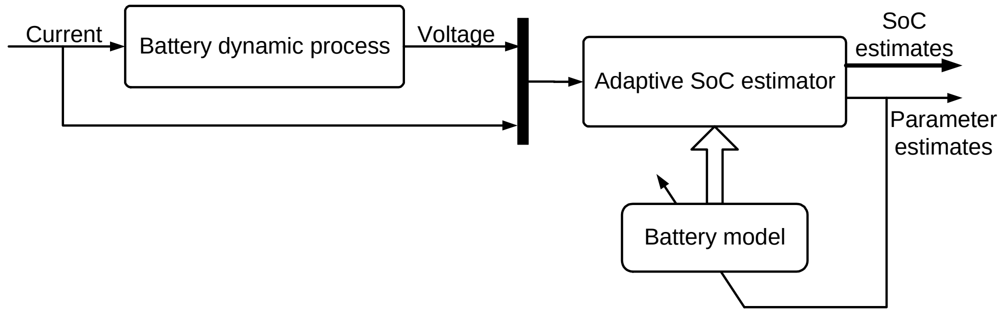


Figure 1: A schematic description of adaptive SoC estimation.

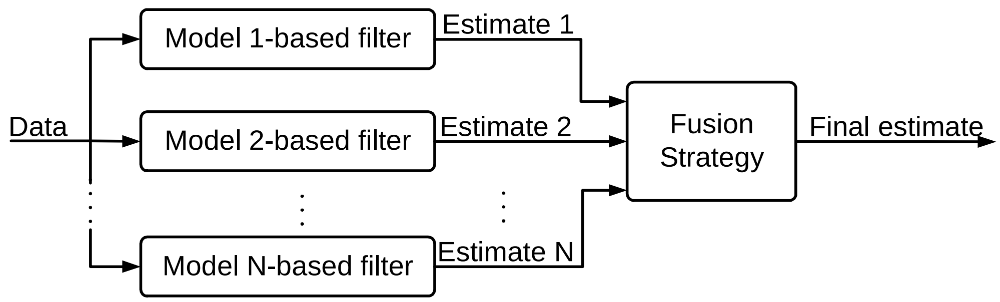


Figure 2: The structure of a multi-model estimator.

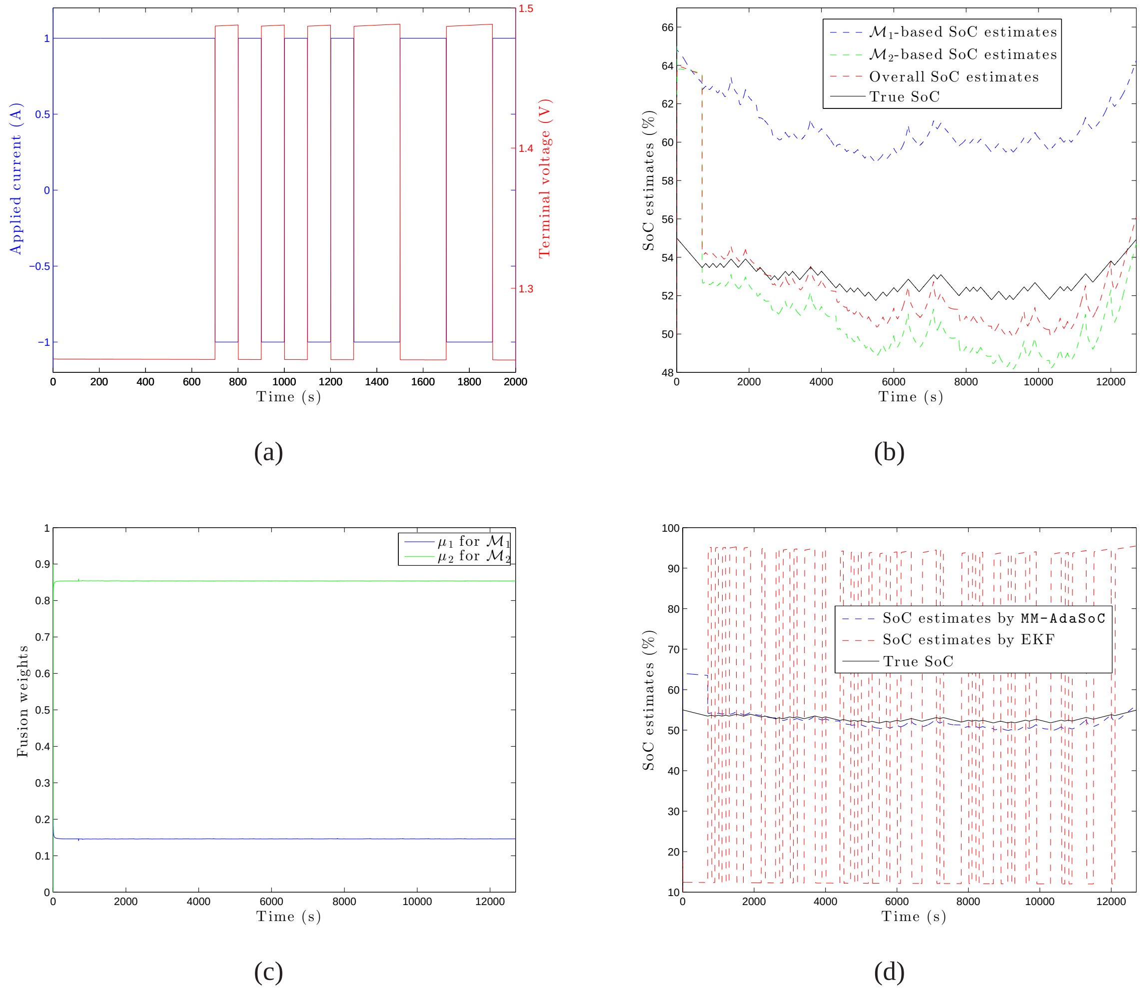


Figure 3: (a) The input current-output voltage profile; (b) SoC estimates versus truth over time; (c) fusion weights for $\mathscr{M}_1$ and $\mathscr{M}_2$ versus time; (d) comparison with the EKF.

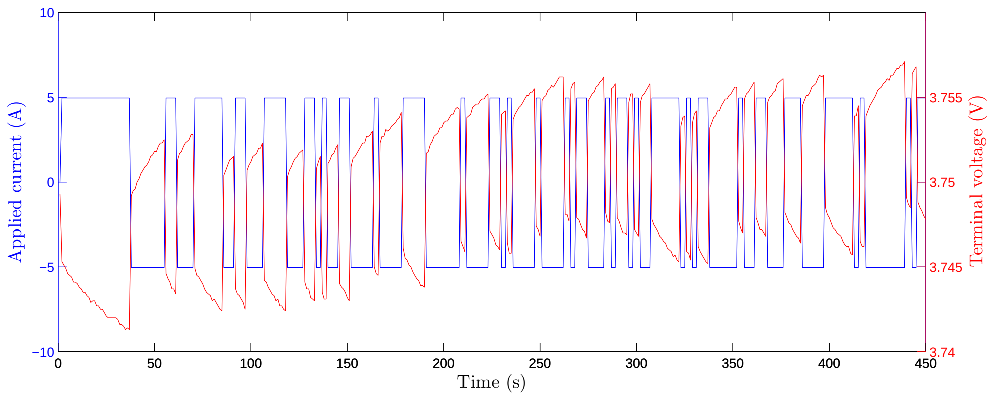


Figure 4: The input-output (current-voltage) profile.

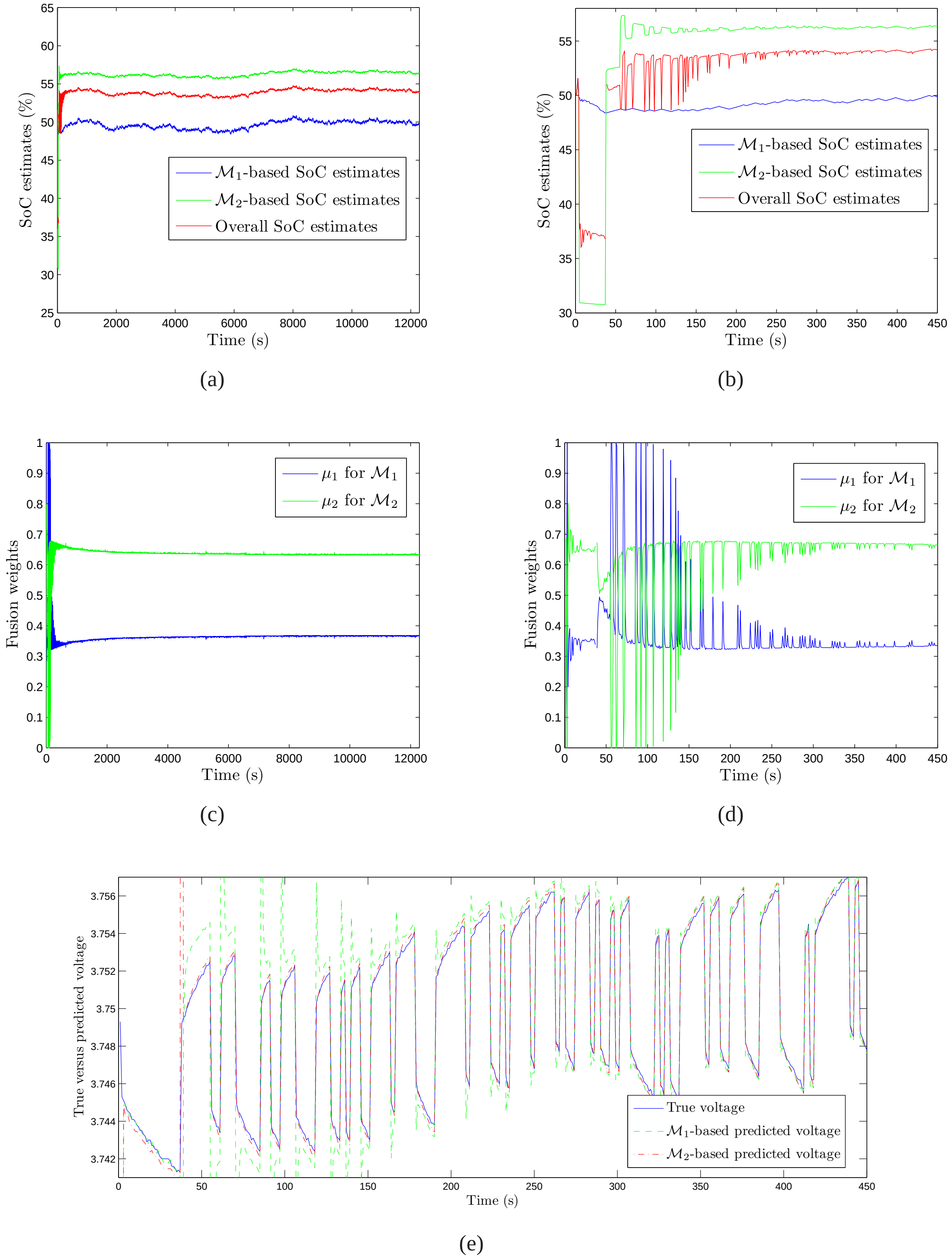


Figure 5: (a) SoC estimates versus time; (b) SoC estimates during the initial 450s; (c) fusion weights for $\mathscr{M}_1$ and $\mathscr{M}_2$ versus time; (d) fusion weights during the initial 450s; (e) comparison between the true and the one-step-forward predicted voltage.